Collective Effects and Self-Consistent Energetic Particle Dynamics in Advanced Tokamaks

F. Zonca 1), S. Briguglio 1), L. Chen 2), G. Fogaccia 1), G. Vlad 1)

1) ENEA C. R. Frascati, C.P. 65, 00044 Frascati, Rome, Italy
2) Department of Physics and Astronomy, University of California, Irvine, CA 92717-4575

e-mail contact of main author: zonca@frascati.enea.it

Abstract. In the present paper, we address the issue of fast ion and fusion product transport in conditions that are typically relevant for burning plasmas operating in so called *Advanced Tokamak* regimes. Our results have direct implications, e.g., on the choice of current profiles for ITER steady state operations. We demonstrate that in a Tokamak equilibrium with hollow-q profile, in general, two types of EPM (Energetic Particle Modes [1]) gap modes may exist near the minimum-q surface ($q = q_0$), characterized by opposite signature in frequency: one with upwards chirping frequency [2] and the other with downward chirping frequency as q_0 drops. It is shown that EPM gap modes are described by the same dispersion relation of the usual resonant EPMs [1] and that they can indeed be considered as the same mode with, however, different dominant damping mechanisms. This work also presents a discussion of EPM non-linear dynamics with respect to energetic ion transport in tokamaks with hollow q-profiles. Numerical simulations based on a Hybrid MHD-Gyrokinetic Code (HMGC) [3, 4], demonstrate that, above the EPM excitation threshold, fast radial redistribution of energetic ions takes place on a time scale that is proportional to the inverse EPM growth rate (typically $\approx 100\tau_A$, $\tau_A = R_0/v_A$ being the Alfvén time). The rapid evolution of EPM mode structures and the associated fast ion transport is interpreted within the framework of the *relay runner* model for non-linear EPM dynamics [5]. It is found that a *sensitive* parameter for tokamak equilibria with hollow-q profiles is q at the minimum-q surface, higher q corresponding to larger particle transport. This fact has clear implications on the choice of current profiles in a burning plasma [6].

1. Introduction

From the point of view of EPM excitations, the plasma cross section in tokamaks with hollow q-profiles is divided into three regions by the presence of the minimum-q surface [7]. Inner and outer regions are obviously characterized by different values of magnetic shear and fusion products/fast ion energy density. The plasma volume inside the minimum-q surface has typically negative and often small shear. Here, the fast ion energy density is maximum, due to the spatial localization of DT fusion cross section and of additional power input sources. Meanwhile, the outer region has positive magnetic shear but small fast ion energy density. A toroidal annulus, centered at the minimum-q surface, separates these two regions and is characterized by peculiar properties of both EPM stability and mode structures. For a wave of toroidal mode number n, it is possible to show that the width of the annulus is given by the inequality $s^2 \lesssim S^2/n$. Here, $s \equiv rq'/q$ is the conventional definition of magnetic shear, *prime* denotes derivation in the radial direction r and $S^2 \equiv r_0^2 q''(r_0)/q_0^2$ is a measure of the concavity of the q-profile at the radial location of the minimum-q surface, where $r = r_0$, $q = q_0$ and $s \to 0$. In this paper, we discuss the relationship of EPMs that are resonantly driven in the small but finite shear region with those that are excited in the toroidal annulus at r_0. Various relevant aspects in this problem, involving both linear (Section 2) and non-linear physics issues (Section 3), will be treated in the present paper.

2. Excitation of resonant EPMs and EPM gap modes

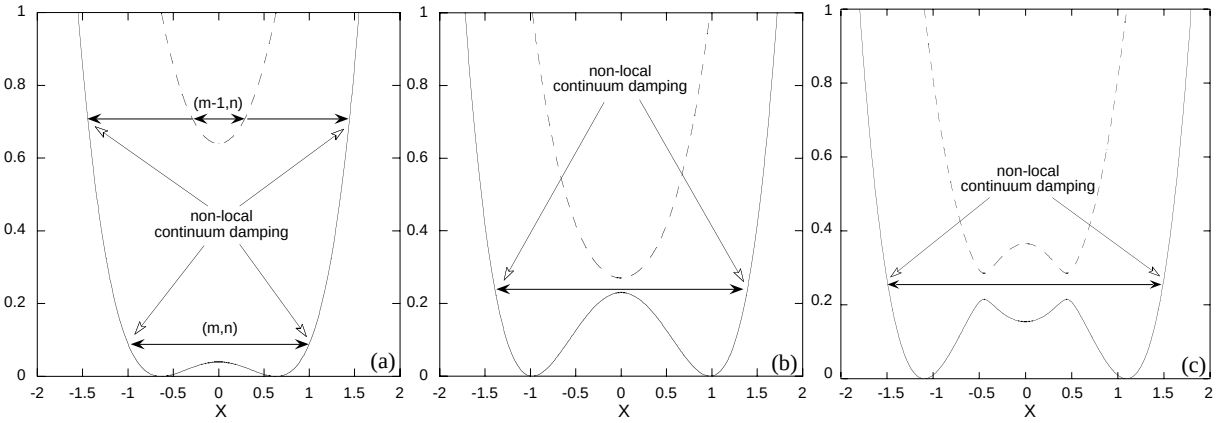

FIG. 1. Structure of the shear Alfvén continuous spectrum near the minimum-q surface at r_0. From (a) to (c), the value of q_0 decreases. Here, $x \equiv \sqrt{nq_0''}(r - r_0)$.

Consider modes localized near r_0, where q has a minimum given by q_0. Consider also a given toroidal mode number n and a poloidal mode number m such that the normalized parallel wave vectors $\Omega_{A,m} \equiv nq_0 - m < 0$ and $\Omega_{A,m-1} \equiv nq_0 - m + 1 > 0$. It is then readily demonstrated that the condition under which continuum damping is minimized is that with $-1/2 < \Omega_{A,m} < 0$ and $1/2 < \Omega_{A,m-1} < 1$. In fact, this is the condition under which there is a frequency gap between the (m, n) mode continuum, that has a local maximum at r_0, and the $(m-1, n)$ mode continuum, that has a local minimum at r_0. For $\Omega_{A,m} + \Omega_{A,m-1} \gg r_0/R_0$, the local ($r \simeq r_0$) structure of the shear Alfvén continuous spectrum is shown in Fig. 1(a). There, it is evident that the typical frequency gap between the local minimum of the $(m-1, n)$ mode continuum and the local maximum of the (m, n) mode continuum is larger than the frequency shift due to toroidal coupling. Thus, toroidal coupling between (m, n) and $(m-1, n)$ modes can be neglected. The two modes, then, satisfy the following approximate dispersion relations, derived from a variational principle [7]:

$$\sqrt{\Omega_{A,m} + \Omega} = \frac{S\pi}{2^{5/2} n^{1/2}} \left(\frac{2n}{S^2} \frac{\Lambda_m}{\Omega_{A,m}} - 1 \right) \ ,$$
$$\sqrt{\Omega_{A,m-1} - \Omega} = \frac{S\pi}{2^{5/2} n^{1/2}} \left(\frac{2n}{S^2} \frac{\Lambda_{m-1}}{\Omega_{A,m-1}} - 1 \right) \ , \qquad (1)$$

where $\Omega \equiv \omega/\omega_A$, $\omega_A = v_A/qR_0$, v_A is the Alfvén speed, R_0 is the tokamak major radius, and Λ_{m-1}, Λ_m represent the resonant and non-resonant contribution of energetic particles. Equations (1) demonstrate that *EPM gap modes* can be excited near a minimum-q surface only in the presence of an energetic ion population [2, 7]. They are valid for general fast ion distribution functions; however, as JET experimental results with Ion Cyclotron Resonant Heating (ICRH) in reversed magnetic shear discharges have recently attracted significant attention [2], in the rest of this Section we will refer to such conditions, specifying Λ_m as

$$\Lambda_m \simeq -\frac{q^2 R_0^2}{m^2/r_0^2} \left(\frac{r_0}{R_0} \right)^{1/2} v_{TH}^3 \frac{8}{\pi} \int_0^\infty \frac{dz}{1+z^2} \int_0^\infty w^{1/2} dw \int_0^\pi d\theta_b \sin\theta_b \mathbf{K}\left(\sin(\theta_b/2)\right)$$
$$\times \frac{4\pi\omega}{c^2} \frac{e_H^2}{m_H} J_0^2\left(\lambda_H\right) Q F_{0H} \sum_h J_h^2\left(\lambda_{BH}\right) \frac{\bar{\omega}_{dH} + h\omega_{BH}}{\bar{\omega}_{dH} + h\omega_{BH} - \omega} \ . \qquad (2)$$

Here, $\mathbf{K}(\sin(\theta_b/2))$ is the complete elliptic integral of the first kind, $J_h,\ \ h=1,2,3,\ldots$ are Bessel functions, θ_b is the trapped particle bounce angle, $v_{TH}\equiv\sqrt{T_H/m_H}$ is the fast tail ion thermal speed, $w\equiv v^2/2v_{TH}^2$, $\lambda_H=\sqrt{2w}k_\theta\rho_{LH}\sqrt{1+z^2}$, $\rho_{LH}=v_{TH}/\omega_{cH}$, $\omega_{cH}=e_HB/m_Hc$, $\lambda_{BH}=\sqrt{wR_0/r_0}\theta_b z q_0 k_\theta\rho_{LH}$, $\bar{\omega}_{dH}=k_\theta\rho_{LH}(v_{TH}/R_0)w$ and the bounce frequency $\omega_{BH}=\sqrt{wr_0/R_0}(v_{TH}/q_0R_0)$. Moreover, integration in z accounts for the *non-local* response of fast ions due to finite Larmor and banana orbit widths, $QF_{0H}=\left(2\omega\partial/\partial v^2+\mathbf{k}\times\mathbf{b}\cdot\nabla/\omega_{cH}\right)F_{0H}$, $\mathbf{b}=\mathbf{B}/B$, and F_{0H} is the fast ion tail distribution function.

Note that the first of Eqs. (1) was originally derived in Ref. [2], where the expression of Λ_m was obtained assuming that the fast ion toroidal precession frequency, $\bar{\omega}_{dH}$, is such that $\bar{\omega}_{dH}\gg\omega$ [2]. In this limit, which applies in a variety of JET experimental conditions [2], the non-resonant fast ion response dominates, $\Lambda_{m-1}/\Omega\simeq\Lambda_m/\Omega<0$, and Eqs. (1) predict that only the (m,n) mode can be excited just above the local maximum in the Alfvén continuum (Fig. 1(a)). A remarkable experimental evidence of this fact is the observation of *Alfvén Cascades* at JET, which are characterized by *upwards chirping* frequencies as the value of q_0 drops due to current diffusion [2]. In general, however, the the $(m-1,n)$ EPM gap mode can also be excited just below the local minimum in the Alfvén continuum, and that would be characterized by *downwards chirping* frequencies as the value of q_0 drops. Generally, a transition from $\mathbb{R}\mathrm{e}\Lambda_m<0$ to $\mathbb{R}\mathrm{e}\Lambda_m>0$ results in a transition from the (m,n) EPM to the the $(m-1,n)$ EPM gap mode excitation [7]. Equation (2) shows that $\mathbb{R}\mathrm{e}\Lambda_m$ depends, among other parameters, both on the velocity ratio v_{TH}/v_A and on the mode frequency. Experimental control on the velocity ratio makes it possible to excite either one of the two EPM gap modes, as described by Eqs. (1). However, the resonant energetic ion response (mode drive) also plays a crucial role. Thus, (m,n) and $(m-1,n)$ EPM gap mode excitations are not mutually exclusive, and we could generally expect the *simultaneous* observation of both *upwards* and *downwards chirping* frequencies as the value of q_0 drops. Depending on the experimental parameter range, one or the other signature should dominate.

As $\Omega_{A,m}+\Omega_{A,m-1}\rightarrow 0^+$ (which may occur when q_0 drops), toroidal coupling effects become more important (cf. Fig. 1(b)). The main modification of Eqs. (1) in this case is due to the existence, at $r=r_0$, of four nearly degenerate shear Alfvén waves at the frequency of the toroidal gap in the Alfvén continuous spectrum. For detailed analyses we refer to Ref. [7], where the EPM gap mode properties are discussed also when $\Omega_{A,m}+\Omega_{A,m-1}\ll -r_0/R_0$, due - *e.g.* - to a further drop in q_0, with the radial structure of the continuous spectrum becoming that of Fig. 1(c). In this case, the EPM *gap mode* smoothly changes from a radial structure localized near $x=\sqrt{nq_0''}(r-r_0)=0$ and will eventually end up into a double-hump structure. This result can be obtained analytically and, anticipating the numerical simulation results of Section 3.2, is also evident from the radial structure of the Fourier harmonics in Fig. 8 (right).

The existence condition of EPM gap modes is that of vanishing *local continuum damping*, *i.e.* that the l.h.s. of Eqs. (1) be real and positive definite. Dominant damping mechanisms are, in this case, either kinetic, as radiative or ion Landau damping, or fluid, as *nonlocal continuum damping*, which is a result of resonant excitation of the Alfvén continuum away from r_0 as it is shown in Figs. 1. Figures 1 also suggest that non-local continuum damping should depend on the mode frequency and, more precisely, decrease for increasing Ω. In fact, as it is demonstrated

in Ref.[7], including this damping mechanism modifies the (m, n) mode dispersion relation into:

$$\sqrt{\Omega_{A,m}+\Omega}\left[1+\mathrm{i}\exp\left(-4\sqrt{-n\Omega_{A,m}}/S\right)\right]=\frac{S\pi}{2^{5/2}n^{1/2}}\left(\frac{2n}{S^2}\frac{\Lambda_m}{\Omega_{A,m}}-1\right)\quad . \tag{3}$$

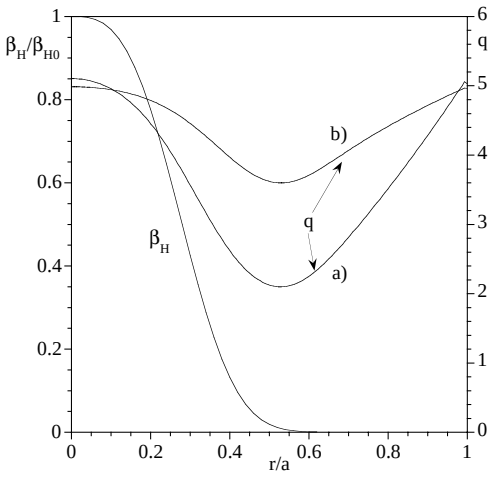

FIG. 2. Equilibrium fast-particle normalized pressure and q-profiles.

From this expression, we note that non-local continuum damping is important at low frequency and that it becomes exponentially small for increasing $-\Omega_{A,m}$. When the complex frequency shift due to energetic particles becomes comparable with the distance of the real mode frequency from the Alfvén continuum accumulation point, the l.h.s. of Eqs. (1) cannot any longer be assumed as real and positive definite. *Local continuum damping* is then finite and the mode acquires the character of a *resonant EPM* [1]. Thus, resonant EPMs and EPM gap modes are indeed the same mode but with different dominant damping mechanisms. Resonant EPMs are generally excited at the radial position where the fast ion drive, $\propto \alpha_H \equiv -R_0 q^2 \beta'_H$, is strongest, *i.e.* typically inside the minimum-q surface where $s<0$. The toroidal annulus of width $\approx (nq''_0)^{-1/2}$, centered at r_0, and the small but finite negative shear region inside it can be treated within a unified mathematical formalism, yielding the same dispersion relation for resonant EPMs and EPM gap modes, which is valid for $s=0$ as well as $0<|s|<1$ [7]:

$$\sqrt{(\Omega^2_{A,m}-\Omega^2)/\Theta_m}=(\pi/4)\left(2\Lambda_m/\Theta_m-1\right)\quad , \tag{4}$$

where $\Theta_m = s^2$ and $\Omega_{A,m}=0$ for $s\neq 0$, and $\Theta_m = S^2\Omega_{A,m}/n$ for $s=0$.

3. Non-linear EPM dynamics and fast-particle transport

In the present section, we analyze EPM non-linear dynamics with respect to both saturation mechanisms and energetic particle transport by means of numerical simulation results obtained with the Hybrid MHD Gyrokinetic code HMGC [3]. Here, we assume plasma equilibria with shifted circular magnetic flux surfaces and an isotropic Maxwellian with constant temperature profile for the velocity space distribution function of energetic ions. Furthermore, for the sake of simplicity, in the specific simulations presented here, we consider full nonlinear wave-particle interactions only, while neglecting nonlinear mode-mode couplings among different toroidal mode numbers n. Fixed simulation parameters are $n=4$, $a/R_0=0.1$ (with a the minor radius of the torus), $\rho_{LH}/a=0.01$, $v_{TH}/v_A|_{r=0}=1$ (energetic ion thermal speed normalized to the Alfvén velocity, on-axis value), and energetic and thermal ion species are assumed to have the same mass number.

The energetic ion radial pressure profile, used in the present analyses, is shown in Fig. 2, where β_H is the ratio of fast-ion and equilibrium magnetic field energy densities and β_{H0} indicates its value on the magnetic axis. The peaking factor, $\beta_{H0}/\langle\beta_H\rangle$, for such profile is $\beta_{H0}/\langle\beta_H\rangle=9.2$, where the volume averaged β_H is defined as $\langle\beta_H\rangle = 2\int_0^1 (r/a)\beta_H d(r/a)$. The two *model* q profiles, employed in the simulations, are also shown in Fig. 2. These profiles do not *realistically*

refer to specific plasma equilibria, as *e.g.* ITER, and they were chosen in order to investigate the role of q-profile parameters which are most relevant for energetic ion transport.

3.1. EPM excitation at different radial locations

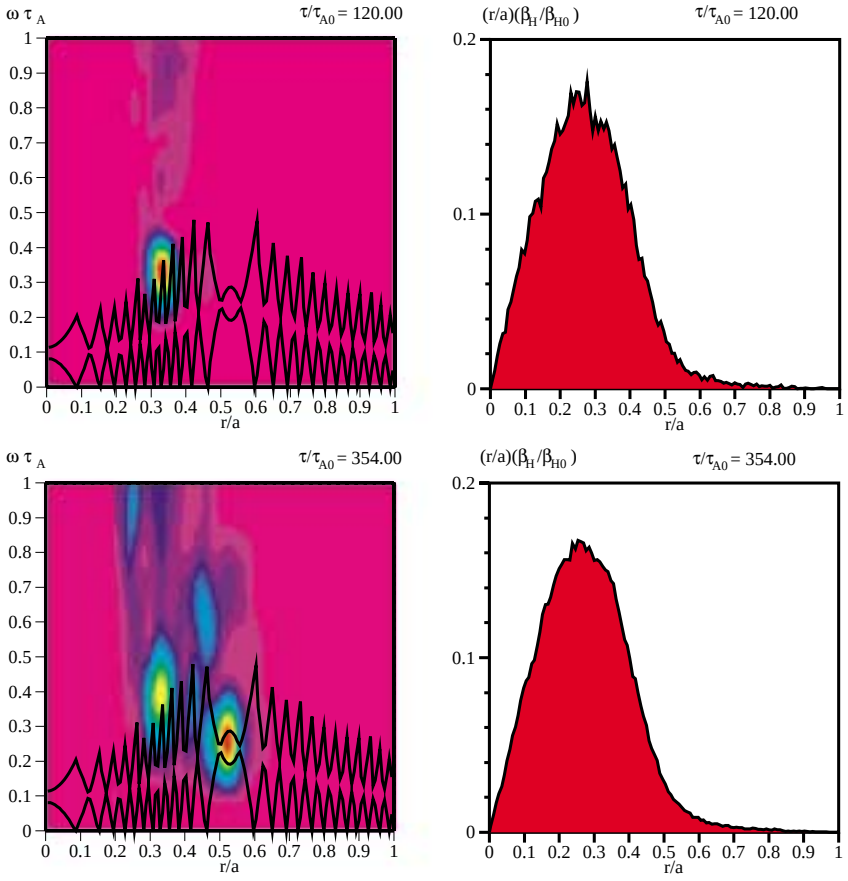

FIG. 3. Power spectrum and energetic-ion line pressure profile at two different times: linear growth phase (top; $\tau = 120\tau_{A0}$) and saturated phase (bottom; $\tau = 354\tau_{A0}$).

For sufficiently peaked pressure profiles, non-linear simulations confirm that resonant EPMs are destabilized at the radial location where α_H is maximum [7]. Numerical results show that non-linearly saturated states are always characterized by EPM gap modes at the minimum-q surface, even when resonant EPMs are excited within the minimum-q surface. Scenarii that yield these time-*asymptotic* saturated conditions continuously vary between two limiting cases [7]. Close to marginal stability, the transport time scale of energetic ions is longer than the inverse growth rate of both resonant EPMs and EPM gap modes excited at r_0. In these conditions, EPM excitations at different radial locations are well described within the theoretical formulation of Section 2, and the modes are characterized by independent non-linear evolutions. This situation is depicted in Fig. 3, where the power spectrum $\sum_m |\phi_{m,n}(r,\omega)|^2$ in the $(r/a, \omega\tau_{A0})$ plane and the energetic-ion line pressure profile, $(r/a)\beta_H(r)/\beta_{H0}$, are shown at two different times: linear growth phase (top; $\tau = 120\tau_{A0}$) and saturated phase (bottom; $\tau = 354\tau_{A0}$). Here, $\tau_{A0} = R_0/v_A|_{r=0}$. The q profile (a) of Fig. 2 and $\beta_{H0} = 0.010$ have been assumed along with a radially constant thermal-plasma density, corresponding to a radially constant Alfvén velocity.

For strong drive, rapidly evolving resonant EPMs are radially displacing the fast ion source towards the position where it can more easily destabilize weaker EPM gap modes. In this second case, the characteristic time scale of EPM gap mode growth is longer than that of fast ion transport: linear stability analyses are, thus, inadequate and the problem is intrinsically non-linear, as it can be seen in Fig. 4 below. [6, 7].

3.2. Fast ion Internal Transport Barrier and avalanches.

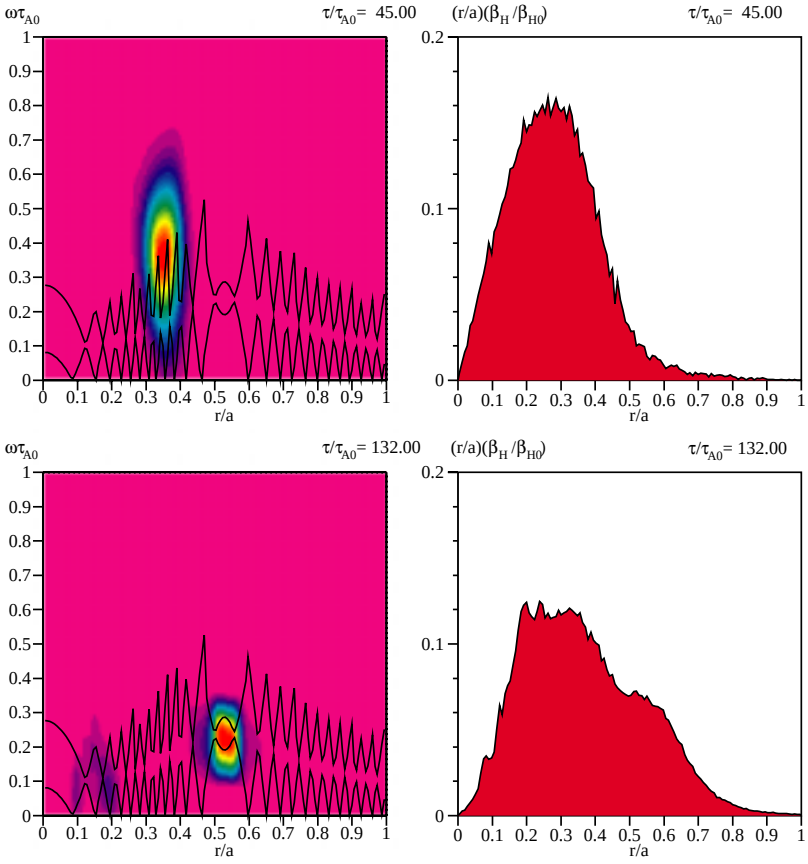

FIG. 4. Linearly unstable (top) and saturated (bottom) phases for $\beta_{H0} = 0.025$ *and the other parameters as in Fig. 3.*

In Fig. 4, an unstable EPM [1], is excited inside the upper continuum (top) by the resonant interaction with energetic ions. Its saturation takes place because of a strong, convective, radial displacement of the energetic ions. The maximum of the power spectrum then migrates in frequency towards the toroidal gap and radially outwards. This occurs because the mode follows the outward-moving β_H maximum gradient and properly readjusts its frequency in order to minimize continuum damping [6].

The fact that the rapid fast-particle radial redistribution stops at the minimum-q surface [6], suggests the existence of an energetic-particle Internal Transport Barrier (ITB), analogous to that of the thermal plasma, for which the presence of a weak or negative magnetic shear region has the effect of reducing the local transport coefficients. The *robustness* of such fast ion ITB can be seen in Fig. 5, where, for the q profile (a) of Fig. 2, the time-asymptotic energetic particle radial distribution is not drastically altered with respect to that of Fig. 4 despite that the drive has been increased by a factor two, $\beta_{H0} = 0.05$. Meanwhile, the properties of the fast-ion ITB crucially depend on the q profile [6]. Figure 6, in fact, shows the simulation results in the saturation phase for the q profile (b) of Fig. 2 and the other parameters same as in Fig. 4. There, the detrimental effect on both local and global energetic ion confinement is macroscopic. In fact, the effect of increasing β_{H0} or modifying the q-profile on fast ion transport is clearly visible in Fig. 7, where the fraction of particles confined within a given flux surface is shown at initial equilibrium conditions (a) and in the time-asymptotic non-linearly saturated phase for Figs. 4 (bottom), 5, and 6 (curves b, c and d, respectively). Here, the definition of the fraction of particles confined within a given flux surface is $2\langle\beta_H\rangle^{-1}\int_0^{r/a}(r/a)\beta_H d(r/a)$, since it coincides with the fraction of confined energy for the present assumption of constant fast ion temperature profile. The time-asymptotic fraction of energetic particles confined within the minimum-q surface located at $r_0/a = 0.525$, which at equilibrium is 99.8% (cf. Fig. 2), is 79% in the case of Fig. 4 and 65% in that of Fig. 5. The global particle losses in the two cases are, respectively, 1.3% and 3.1%, indicating that particle

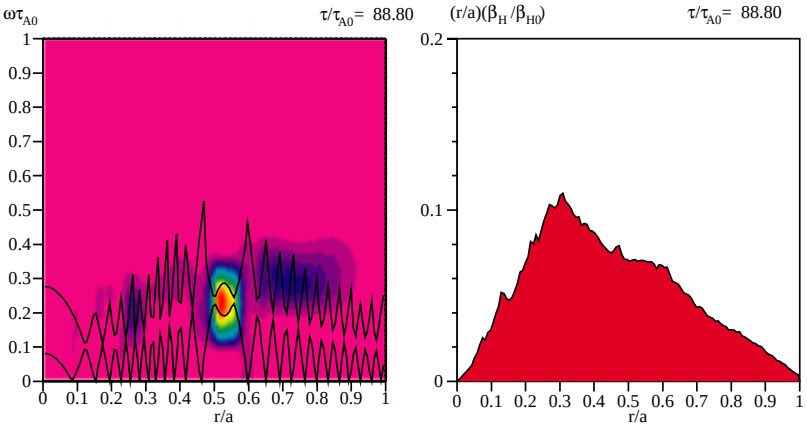

FIG. 5. Saturated phase for $\beta_H(0) = 0.05$ and the other parameters as in Fig. 3

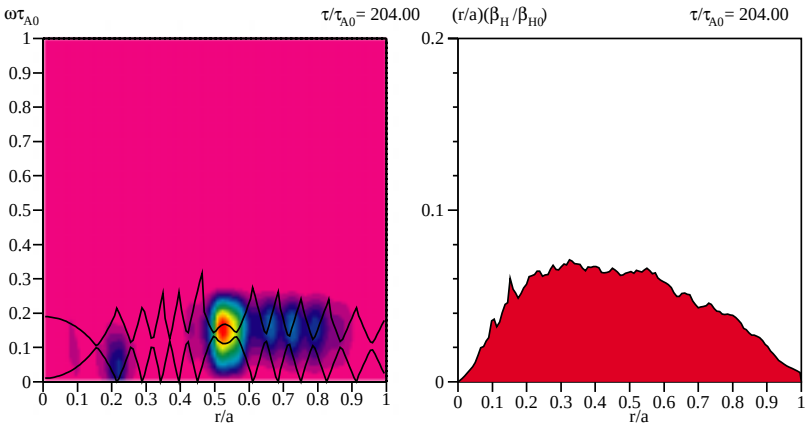

FIG. 6. Saturated phase for the q profile (b) of Fig. 2. Other parameters as in Fig. 4.

transport results mainly in radial particle redistribution. On the contrary, in the case of Fig. 6, global particle losses are 6.6%, and the time-asymptotic fraction of fast-ions confined within the minimum-q surface is 56%. These results clearly indicate that profiles with lowest q_{min} (above $q_{min} = 2$ for MHD stability reasons) and highest q'' exhibit the best confinement properties of fast ions [6]. The reason for this is that, for a given value of β'_H, the mode radial width scales, near the q_{min} surface, as $1/\sqrt{nq''}$ [7], while the typical orbit size is proportional to q_{min}. Decreasing the hollowness of the q profile, while taking $q(0)$ and $q(a)$ fixed, yields lower q'' and larger q_{min} values, and makes both the mode and the orbit widths larger than in the deeply-hollow q-profile case. Moreover, the energetic-ion drive intensity, α_H, scales as q^2_{min}. The mode is then a more efficient scattering source for energetic-ion orbits even in the relatively low β_H case (as in Fig. 6 for $\beta_{H0} = 0.025$). All these facts provide useful insights into the fundamental properties of fast-ion ITB at the minimum-q surface and have clear implications on the choice of current profiles in a burning plasma, suggesting that good confinement of fusion products will set constraints on the maximum radial location of the minimum-q surface and on the value of q_{min} [6]. The simulation results in Figs. 4-6 also shed some light on the characteristic properties of energetic particle transport when resonant EPMs are strongly excited. In fact, there is evidence that non-linear EPM dynamics produces an *avalanche*, *i.e.* the radial displacement of an *unstable propagating front* associated with rapid fast-particle radial redistribution which stops at the minimum-q surface [6]. That this phenomenology

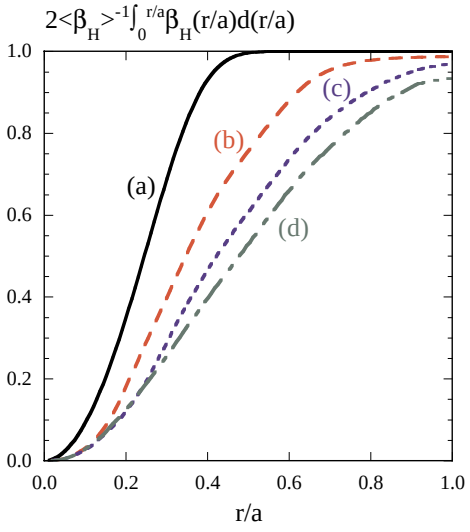

FIG. 7. Fraction of particles confined within a given flux surface at equilibrium (a), compared to that of Fig. 4 (b), Fig. 5 (c) and Fig. 6 (d).

occurs during EPM induced energetic particle transport is shown in Fig. 8. There, three successive time-frames are shown, which are taken from Fig. 4 simulation results in order to display the radial mode structure evolution during the linear destabilization and non-linear saturation phases. Different Fourier harmonics, $|\phi_{m,n}|$, are displayed in different colors. As reference, the α_H deviation from the initial equilibrium profile, $\delta\alpha_H$, is also shown as it results due to the non-linear EPM fluctuations. It is evident that the *mixture* of poloidal harmonics that give the global mode structure is changing in time as the fast-ion source is radially displaced, exactly as it is conjectured in the *relay runner model* [5]. This model is a paradigm for strongly excited resonant EPMs non-linear evolution. It is based on the *mode particle pumping* mechanism [8] and assumes that each dominant mode (poloidal harmonic [1]) displaces energetic ions radially and eventually becomes subdominant, replaced by the next mode in the same fashion as different *runners* do in a *relay race*. The agreement between simulation results of Fig. 8 and the paradigm model is remarkable.

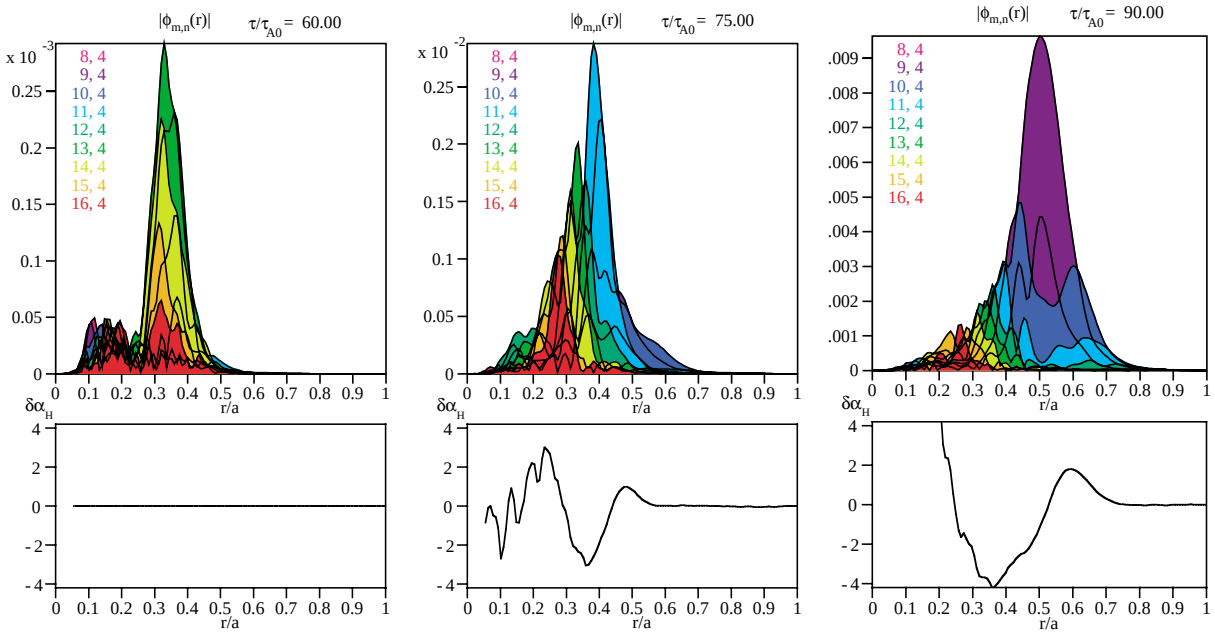

FIG. 8. EPM radial structure and its various poloidal Fourier harmonic components are shown at three different times, $\tau = 60\tau_{A0}$ (left), $\tau = 75\tau_{A0}$ (center) and $\tau = 90\tau_{A0}$ (right), for the simulation of Fig. 4. The α_H deviation from the initial equilibrium profile, $\delta\alpha_H$, is also shown.

[1] L. Chen, Phys. Plasmas **1**, 1519, (1994).
[2] H. L. Berk *et al.*, Phys. Rev. Lett. **87**, 185002, (2001).
[3] S. Briguglio, G. Vlad, F. Zonca and C. Kar, Phys. Plasmas **2**, 3711, (1995).
[4] S. Briguglio, F. Zonca and G. Vlad, Phys. Plasmas **5**, 3287, (1998).
[5] F.Zonca and L. Chen, in Proceedings of the 6.th IAEA TCM on Energetic Particles in Magnetic Confinement Systems, JAERI-Conf 2000-004, pp. 52-56, (2000).
[6] S. Briguglio, G. Vlad, F. Zonca, G. Fogaccia, Phys. Lett. A **302**, 308, (2002).
[7] F. Zonca, S. Briguglio, L. Chen, S. Dettrick, G. Fogaccia, D. Testa, and G. Vlad, *Energetic Particle Mode Stability in Tokamaks with Hollow q-profiles*, to be published on Phys. Plasmas, (2002).
[8] R.B. White *et al.*, Phys. Fluids **26**, 2958, (1983).

[1] Incidentally, we note that this paradigm works *a fortiori* if different n's are also considered.